

# Revisit of SNLS3 constraints on holographic dark energy: the effects of varying $\beta$ and different light-curve fitters

Shuang Wang,<sup>1,\*</sup> Jia-Jia Geng,<sup>1,†</sup> Yi-Liang Hu,<sup>1,‡</sup> and Xin Zhang<sup>1,2,§</sup>

<sup>1</sup>*Department of Physics, College of Sciences, Northeastern University, Shenyang 110004, China*

<sup>2</sup>*Center for High Energy Physics, Peking University, Beijing 100080, China*

In Phys. Rev. D 88, 043511 (2013), using the Supernova Legacy Survey Three Year (SNLS3) data, Wang & Wang found that there is a strong evidence for the redshift-evolution of color-luminosity parameter  $\beta$ . In this paper, we explore the effects of varying  $\beta$  on the cosmological constraints on holographic dark energy (HDE) model. To break the degeneracy between various model parameters, we include the Planck distance prior data, as well as the latest galaxy clustering (GC) data extracted from SDSS DR7 and BOSS. In addition, We also study the effects of different light-curve fitters on parameter estimation. We find that  $\beta$  deviates from a constant at the  $5\sigma$  level; besides, adding an additional parameter of  $\beta$  can reduce  $\chi^2$  by  $\sim 35$ . This indicates that the evolution of  $\beta$  should be taken into account seriously in the cosmology-fits. We also find that compared to the constant  $\beta$  case, varying  $\beta$  yields a larger  $\Omega_m$ , a larger  $c$  and a smaller  $h$ ; besides, for these two cases, the  $2\sigma$  ranges of parameter space are quite different. This shows that ignoring the evolution of  $\beta$  may cause systematic bias. In addition, we find that compared to the differences between constant  $\beta$  and varying  $\beta(z)$  cases, the effects of different light-curve fitters are very small.

PACS numbers: 98.80.-k, 98.80.Es, 95.36.+x

Keywords: Cosmology, Type Ia supernova, Dark Energy

## I. INTRODUCTION

In the past 15 years, various cosmological observations [1–7] all indicate that the Universe is undergoing an accelerated expansion. This counterintuitive phenomenon may be due to an unknown energy component (i.e., dark energy (DE) [8–21]), or a modification of general relativity (i.e., modified gravity (MG) [22–29]). For recent reviews, see [30–39].

One of the most powerful probes of DE is the use of Type Ia supernovae (SNe Ia) [40–43]. In 2010, a high quality supernova (SN) dataset from the first three years of the Supernova Legacy Survey (SNLS3) was released [44]. Then, Conley et al. (2011; hereafter C11) presented SN-only cosmological results by combining the SNLS3 SNe with various low- to mid- $z$  samples [45], and Sullivan et al. presented the joint cosmological constraints by combining the SNLS3 dataset with other cosmological observations [46]. Depending on different light-curve fitters, C11 presented three SN data sets: “SALT2”, which consists of 473 SNe Ia; “SiFTO”, which consists of 468 SNe Ia; and “Combined”, which consists of 472 SNe Ia. Unlike other SN group, the SNLS team treated two important quantities, stretch-luminosity parameter  $\alpha$  and color-luminosity parameter  $\beta$  of SNe Ia, as free model parameters on the same footing as the cosmological parameters, all to be estimated during the cosmology-fitting process using the covariance matrix that includes *both*

statistical and systematic errors.

One of the most critical challenges is the control of the systematic uncertainties of SNe Ia. Due to the effect of potential SN evolution, there is the possibility for the redshift evolution of  $\alpha$  and  $\beta$  [47–50]. The current studies show that  $\alpha$  is still consistent with a constant. In [51], using the SNLS3 SN data, Wang & Wang found that  $\beta$  increases significantly with  $z$  at the  $5\sigma$  confidence level when systematic uncertainties are taken into account. This conclusion is insensitive to the lightcurve fitter used to derive the SNLS3 sample, or the functional form of  $\beta(z)$  assumed [51]. In [52], using the cosmological constant, the constant  $w$ , and the non-constant  $w$  models, Wang, Li & Zhang showed that a time-varying  $\beta$  has significant impact on parameter estimation; in addition, it was found that considering the evolution of  $\beta$  is helpful in reducing the tension between SN and other cosmological observations. Since we are still in the dark about the nature of DE, it is interesting to further study the effects of varying  $\beta$  on other DE models.

The DE problem may be in essence an issue of quantum gravity [53], and it is believed that the holographic principle is a fundamental principle of quantum gravity [54]. Cohen *et al.* [55] suggested that quantum zero-point energy of a system with size  $L$  should not exceed the mass of a black hole with the same size, i.e.,  $L^3\Lambda^4 \leq LM_{\text{P1}}^2$  (here  $M_{\text{P1}}$  is the reduced Planck mass, and  $\Lambda$  is the ultraviolet (UV) cutoff of the system). Therefore, the UV cutoff of a system is related to its infrared (IR) cutoff. When we consider the whole universe, the vacuum energy related to this holographic principle can be viewed as dark energy, and the corresponding energy density becomes

$$\rho_{\text{de}} = 3c^2 M_{\text{P1}}^2 L^{-2}, \quad (1)$$

where  $c$  is a dimensionless model parameter which mod-

\*Electronic address: wjysyngj@163.com

†Electronic address: gengjiajia163@163.com

‡Electronic address: onebright@163.com

§Electronic address: zhangxin@mail.neu.edu.cn

ulates the DE density [56]. In [56], Li suggested that the IR length-scale cutoff should be chosen as the size of the future event horizon of the universe,  $R_{eh}(t) = a(t) \int_t^{+\infty} dt'/a(t')$ . More generically, when we also consider the spatial curvature in a universe, the IR length cut-off  $L$  takes the form

$$L = ar(t), \quad (2)$$

where

$$r(t) = \frac{1}{\sqrt{k}} \text{sinn} \left( \sqrt{k} \int_t^{+\infty} \frac{dt'}{a(t')} \right), \quad (3)$$

with  $\text{sinn}(x) = \sin(x)$ ,  $x$ , and  $\sinh(x)$  for  $k > 0$ ,  $k = 0$ , and  $k < 0$ , respectively. This leads to the following equation of state (EOS) of DE,

$$w_{de}(z) = -\frac{1}{3} - \frac{2}{3} \sqrt{\frac{\Omega_{de}(z)}{c^2} + \Omega_k(z)}, \quad (4)$$

which can yield an accelerated expanding universe. In Eq. (4), the function  $\Omega_{de}(z)$  is determined by the following coupled differential equation system [57]

$$\frac{1}{E} \frac{dE}{dz} = -\frac{\Omega_{de}}{1+z} \left( \frac{\Omega_k - \Omega_r - 3}{2\Omega_{de}} + \frac{1}{2} + \sqrt{\frac{\Omega_{de}}{c^2} + \Omega_k} \right), \quad (5)$$

$$\frac{d\Omega_{de}}{dz} = -\frac{2\Omega_{de}(1 - \Omega_{de})}{1+z} \left( \sqrt{\frac{\Omega_{de}}{c^2} + \Omega_k} + \frac{1}{2} - \frac{\Omega_k - \Omega_r}{2(1 - \Omega_{de})} \right), \quad (6)$$

where  $E(z) \equiv H(z)/H_0$  is the dimensionless Hubble expansion rate,  $\Omega_k(z) = \Omega_{k0}(1+z)^2/E(z)^2$ , and  $\Omega_r(z) = \Omega_{r0}(1+z)^4/E(z)^2$ . In addition,  $\Omega_{r0} = \Omega_{m0}/(1+z_{eq})$ , and  $z_{eq} = 2.5 \times 10^4 \Omega_{m0} h^2 (T_{cmb}/2.7 \text{ K})^{-4}$  (here we take  $T_{cmb} = 2.7255 \text{ K}$ ). The initial conditions are  $E(0) = 1$  and  $\Omega_{de}(0) = 1 - \Omega_{m0} - \Omega_{k0} - \Omega_{r0}$ .

The holographic dark energy (HDE) model described above is a physically plausible dark energy candidate. It has been widely studied both theoretically [58] and observationally [59]. In this paper, we study the effects of varying  $\beta$  on the SNLS3 constraints of the HDE model. In addition, it is also very interesting to discuss the effects of different light-curve fitters on parameter estimation. To break the degeneracy between various model parameters, we also use the Planck distance prior data [60], as well as the latest galaxy clustering (GC) data extracted from SDSS DR7 [61] and BOSS [62].

We describe our method in Sec. II, present our results in Sec. III, and conclude in Sec. IV. In this paper, we assume today's scale factor  $a_0 = 1$ , thus the redshift  $z = a^{-1} - 1$ . The subscript "0" always indicates the present value of the corresponding quantity, and the natural unit is used.

## II. METHOD

### A. SN Ia Data

The comoving distance to an object at redshift  $z$  is given by

$$r(z) = H_0^{-1} |\Omega_{k0}|^{-1/2} \text{sinn}[|\Omega_{k0}|^{1/2} \Gamma(z)], \quad (7)$$

where  $\Gamma(z) = \int_0^z \frac{dz'}{E(z')}$ , and  $\text{sinn}(x) = \sin(x)$ ,  $x$ ,  $\sinh(x)$  for  $\Omega_{k0} < 0$ ,  $\Omega_{k0} = 0$ , and  $\Omega_{k0} > 0$  respectively.

SN Ia data give measurements of the luminosity distance  $d_L(z)$  through that of the distance modulus of each SN:

$$\mu_0 \equiv m - M = 5 \log \left[ \frac{d_L(z)}{\text{Mpc}} \right] + 25, \quad (8)$$

where  $m$  and  $M$  represent the apparent and absolute magnitude of an SN. Moreover, the luminosity distance  $d_L(z) = (1+z)r(z)$ .

Here we use the SNLS3 data set. As mentioned above, based on different light-curve fitters, three SN sets of SNLS3 are given, including "SALT2", "SIFTO", and "Combined". To perform a comparative study, all these three sets will be used in this paper.

In [51], by considering three functional forms (linear case, quadratic case, and step function case), Wang & Wang showed that the evolutions of  $\alpha$  and  $\beta$  are insensitive to functional form of  $\alpha$  and  $\beta$  assumed. So in this paper, we just adopt a constant  $\alpha$  and a linear  $\beta(z) = \beta_0 + \beta_1 z$ . Now, the predicted magnitude of an SN becomes

$$m_{\text{mod}} = 5 \log_{10} \mathcal{D}_L(z|\mathbf{p}) - \alpha(s-1) + \beta(z)\mathcal{C} + \mathcal{M}, \quad (9)$$

where  $\mathcal{D}_L(z|\mathbf{p})$  is the luminosity distance multiplied by  $H_0$  for a given set of cosmological parameters  $\{\mathbf{p}\}$ ,  $s$  is the stretch measure of the SN light curve shape, and  $\mathcal{C}$  is the color measure for the SN.  $\mathcal{M}$  is a nuisance parameter representing some combination of the absolute magnitude of a fiducial SN,  $M$ , and the Hubble constant,  $H_0$ . Now we have

$$\mathcal{D}_L(z|\mathbf{s}) \equiv H_0(1+z_{\text{hel}})r(z|\mathbf{s}), \quad (10)$$

where  $z$  and  $z_{\text{hel}}$  are the CMB restframe and heliocentric redshifts of SN.

For a set of  $N$  SNe with correlated errors, we have [45]

$$\chi^2 = \Delta \mathbf{m}^T \cdot \mathbf{C}^{-1} \cdot \Delta \mathbf{m} \quad (11)$$

where  $\Delta \mathbf{m} \equiv m_B - m_{\text{mod}}$  is a vector with  $N$  components,  $m_B$  is the rest-frame peak B-band magnitude of the SN, and  $\mathbf{C}$  is the  $N \times N$  covariance matrix of the SN. Note that  $\Delta \mathbf{m}$  is equivalent to  $\Delta \mu_0$ , since

$$\Delta \mathbf{m} \equiv m_B - m_{\text{mod}} = [m_B + \alpha(s-1) - \beta(z)\mathcal{C}] - \mathcal{M}. \quad (12)$$

The total covariance matrix is [45]

$$\mathbf{C} = \mathbf{D}_{\text{stat}} + \mathbf{C}_{\text{stat}} + \mathbf{C}_{\text{sys}}, \quad (13)$$

with the diagonal part of the statistical uncertainty given by [45]

$$\begin{aligned} \mathbf{D}_{\text{stat},ii} &= \sigma_{m_B,i}^2 + \sigma_{\text{int}}^2 + \sigma_{\text{lensing}}^2 + \sigma_{\text{host correction}}^2 \\ &+ \left[ \frac{5(1+z_i)}{z_i(1+z_i/2)\ln 10} \right]^2 \sigma_{z,i}^2 \\ &+ \alpha^2 \sigma_{s,i}^2 + \beta(z_i)^2 \sigma_{\mathcal{C},i}^2 \\ &+ 2\alpha C_{m_B s,i} - 2\beta(z_i) C_{m_B \mathcal{C},i} \\ &- 2\alpha\beta(z_i) C_{s\mathcal{C},i}, \end{aligned} \quad (14)$$

where  $C_{m_B s,i}$ ,  $C_{m_B \mathcal{C},i}$ , and  $C_{s\mathcal{C},i}$  are the covariances between  $m_B$ ,  $s$ , and  $\mathcal{C}$  for the  $i$ -th SN,  $\beta_i = \beta(z_i)$  are the values of  $\beta$  for the  $i$ -th SN. Note also that  $\sigma_{z,i}^2$  includes a peculiar velocity residual of 0.0005 (i.e., 150 km/s) added in quadrature [45]. Per C11, here we fix the intrinsic scatter  $\sigma_{\text{int}}$  to ensure that  $\chi^2/dof = 1$ . Varying  $\sigma_{\text{int}}$  could have a significant impact on parameter estimation, see [63] for details.

We define  $\mathbf{V} \equiv \mathbf{C}_{\text{stat}} + \mathbf{C}_{\text{sys}}$ , where  $\mathbf{C}_{\text{stat}}$  and  $\mathbf{C}_{\text{sys}}$  are the statistical and systematic covariance matrices, respectively. After treating  $\beta$  as a function of  $z$ ,  $\mathbf{V}$  is given in the form,

$$\begin{aligned} \mathbf{V}_{ij} &= V_{0,ij} + \alpha^2 V_{a,ij} + \beta_i \beta_j V_{b,ij} \\ &+ \alpha V_{0a,ij} + \alpha V_{0a,ji} \\ &- \beta_j V_{0b,ij} - \beta_i V_{0b,ji} \\ &- \alpha \beta_j V_{ab,ij} - \alpha \beta_i V_{ab,ji}. \end{aligned} \quad (15)$$

It must be stressed that, while  $V_0$ ,  $V_a$ ,  $V_b$ , and  $V_{0a}$  are the same as the ‘‘normal’’ covariance matrices given by the SNLS data archive,  $V_{0b}$ , and  $V_{ab}$  are *not* the same as the ones given there. This is because the original matrices of SNLS3 are produced by assuming that  $\beta$  is constant. We have used the  $V_{0b}$  and  $V_{ab}$  matrices for the ‘‘Combined’’ set that are applicable when varying  $\beta(z)$  (A. Conley, private communication, 2013).

In [51], it is found that the flux-averaging of SNe [64–67] may be helpful to reduce the impact of varying  $\beta$ . It should be mentioned that the results of flux-averaging depend on the choices of redshift cut off  $z_{\text{cut}}$ :  $\beta$  still increases with  $z$  when all the SNe are flux-averaged, and  $\beta$  is consistent with being a constant when only SNe at  $z \geq 0.04$  are flux-averaged [51]. Since the unknown systematic biases originate mostly from low  $z$  SNe, flux-averaging *all* SNe should lead to the least biased results. This means that after applying the flux-averaging method, the problem of varying  $\beta$  is not completely solved. For simplicity, we do not use the flux-averaging method in this paper, and we will discuss the issue of flux-averaging in future work.

## B. CMB and GC data

For CMB data, we use the latest distance prior data extracted from Planck first data release [60].

CMB can give us the comoving distance to the photon-decoupling surface  $r(z_*)$ , and the comoving sound horizon at photon-decoupling epoch  $r_s(z_*)$ . In 2007, Wang & Mukherjee [68] showed that the CMB shift parameters

$$\begin{aligned} R &\equiv \sqrt{\Omega_{m0} H_0^2} r(z_*), \\ l_a &\equiv \pi r(z_*)/r_s(z_*), \end{aligned} \quad (16)$$

together with  $\omega_b \equiv \Omega_b h^2$ , provide an efficient summary of CMB data as far as dark energy constraints go [69].

The comoving sound horizon at redshift  $z$  is given by

$$\begin{aligned} r_s(z) &= \int_0^z \frac{c_s dt'}{a(t')} = cH_0^{-1} \int_z^\infty dz' \frac{c_s}{E(z')}, \\ &= H_0^{-1} \int_0^a \frac{da'}{\sqrt{3(1+\bar{R}_b a') a'^4 E^2(z')}}}, \end{aligned} \quad (17)$$

The sound speed is  $c_s = 1/\sqrt{3(1+\bar{R}_b a)}$ , with  $\bar{R}_b a = 3\rho_b/(4\rho_\gamma)$ ,  $\bar{R}_b = 31500\Omega_{b0}h^2(T_{\text{cmb}}/2.7\text{ K})^{-4}$ , and  $T_{\text{cmb}} = 2.7255\text{ K}$ .

The redshift to the photon-decoupling surface,  $z_*$ , is given by the fitting formula [70],

$$z_* = 1048 [1 + 0.00124(\Omega_{b0}h^2)^{-0.738}] [1 + g_1(\Omega_{m0}h^2)^{g_2}], \quad (18)$$

where

$$g_1 = \frac{0.0783(\Omega_{b0}h^2)^{-0.238}}{1 + 39.5(\Omega_{b0}h^2)^{0.763}}, \quad (19)$$

$$g_2 = \frac{0.560}{1 + 21.1(\Omega_{b0}h^2)^{1.81}}. \quad (20)$$

The redshift of the drag epoch,  $z_d$ , is well approximated by [71]

$$z_d = \frac{1291(\Omega_{m0}h^2)^{0.251}}{1 + 0.659(\Omega_{m0}h^2)^{0.828}} [1 + b_1(\Omega_{b0}h^2)^{b_2}], \quad (21)$$

where

$$b_1 = 0.313(\Omega_{m0}h^2)^{-0.419} [1 + 0.607(\Omega_{m0}h^2)^{0.674}] \quad (22)$$

$$b_2 = 0.238(\Omega_{m0}h^2)^{0.223}. \quad (23)$$

Using the Planck+lensing+WP data, the mean values and covariance matrix of  $\{R, l_a, \omega_b\}$  are obtained [60],

$$\begin{aligned} \langle l_a \rangle &= 301.57, \sigma(l_a) = 0.18, \\ \langle R \rangle &= 1.7407, \sigma(R) = 0.0094, \\ \langle \omega_b \rangle &= 0.02228, \sigma(\omega_b) = 0.00030. \end{aligned} \quad (24)$$

The normalized covariance matrix of  $(l_a, R, \omega_b)$  is

$$\begin{pmatrix} 1.0000 & 0.5250 & -0.4235 \\ 0.5250 & 1.0000 & -0.6925 \\ -0.4235 & -0.6925 & 1.0000 \end{pmatrix}. \quad (25)$$

Then, the covariance matrix for  $(l_a, R, \omega_b)$  is given by

$$\text{Cov}_{CMB}(p_i, p_j) = \sigma(p_i) \sigma(p_j) \text{NormCov}_{CMB}(p_i, p_j), \quad (26)$$

where  $i, j = 1, 2, 3$ . The rms variance  $\sigma(p_i)$  and the normalized covariance matrix  $\text{NormCov}_{CMB}$  are given by Eqs.(24) and (25).

CMB data are included in our analysis by adding the following term to the  $\chi^2$  of a given model with  $p_1 = l_a(z_*)$ ,  $p_2 = R(z_*)$ , and  $p_3 = \omega_b$ :

$$\chi_{CMB}^2 = \Delta p_i [\text{Cov}_{CMB}^{-1}(p_i, p_j)] \Delta p_j, \quad \Delta p_i = p_i - p_i^{data}, \quad (27)$$

where  $p_i^{data}$  are the mean from Eq.(24), and  $\text{Cov}_{CMB}^{-1}$  is the inverse of the covariance matrix of  $[l_a(z_*), R(z_*), \omega_b]$  from Eq.(26).

For GC data, we use the measurements of  $H(z)r_s(z_d)$  and  $D_A(z)/r_s(z_d)$  (where  $H(z)$  is the Hubble parameter,  $D_A(z)$  is the angular diameter distance, and  $r_s(z_d)$  is the sound horizon at the drag epoch) from the two-dimensional two-point correlation function measured at  $z = 0.35$  [61] and  $z = 0.57$  [62]. The  $z = 0.35$  measurement was made by Chuang & Wang [61] using a sample of the SDSS DR7 Luminous Red Galaxies (LRGs). The  $z = 0.57$  measurement was made by Chuang et al. [62] using the CMASS galaxy sample from BOSS.

Using the two-dimensional two-point correlation function of SDSS DR7 in the scale range of 40–120 Mpc/ $h$ , Chuang & Wang (2012) [61] found that

$$\begin{aligned} H(z = 0.35)r_s(z_d) &= 0.0434 \pm 0.0018, \\ D_A(z = 0.35)/r_s(z_d) &= 6.60 \pm 0.26, \\ r &= 0.0604, \end{aligned} \quad (28)$$

where  $r$  is the normalized correlation coefficient between  $H(z = 0.35)r_s(z_d)$  and  $D_A(z = 0.35)/r_s(z_d)$ , and  $r_s(z_d)$  is the sound horizon at the drag epoch [given by Eqs.(17) and (21)].

In a similar analysis using the CMASS galaxy sample from BOSS, Chuang et al. found that [62]

$$\begin{aligned} H(z = 0.57)r_s(z_d) &= 0.0454 \pm 0.0031, \\ D_A(z = 0.57)/r_s(z_d) &= 8.95 \pm 0.27, \\ r &= 0.4874. \end{aligned} \quad (29)$$

We marginalize over the growth rate measurement made by Chuang et al. [62] for a conservative approach.

GC data are included in our analysis by adding  $\chi_{GC}^2 = \chi_{GC1}^2 + \chi_{GC2}^2$ , with  $z_{GC1} = 0.35$  and  $z_{GC2} = 0.57$ , to the  $\chi^2$  of a given model. Note that

$$\chi_{GCi}^2 = \Delta p_i [\text{Cov}_{GC}^{-1}(p_i, p_j)] \Delta p_j, \quad \Delta p_i = p_i - p_i^{data}, \quad (30)$$

where  $p_1 = H(z_{GCi})r_s(z_d)$  and  $p_2 = D_A(z_{GCi})/r_s(z_d)$ , with  $i = 1, 2$ .

TABLE I: A comparison for the fitting results of constant  $\beta$  and linear  $\beta(z)$  cases. The SN(Combined)+CMB+GC data are used in the analysis.

Parameter	constant $\beta$ case	linear $\beta(z)$ case
$\alpha$	$1.448^{+0.0760}_{-0.127}$	$1.416^{+0.097}_{-0.095}$
$\beta_0$	$3.270^{+0.082}_{-0.109}$	$1.403^{+0.359}_{-0.312}$
$\beta_1$	N/A	$5.167^{+0.971}_{-0.967}$
$\Omega_{m0}$	$0.274^{+0.012}_{-0.016}$	$0.288^{+0.015}_{-0.013}$
$c$	$0.687^{+0.057}_{-0.068}$	$0.768^{+0.112}_{-0.068}$
$h$	$0.715^{+0.021}_{-0.014}$	$0.698^{+0.017}_{-0.017}$
$\omega_b$	$0.02232^{+0.00025}_{-0.00030}$	$0.02230^{+0.00027}_{-0.00029}$
$\Omega_{k0}$	$0.0077^{+0.0039}_{-0.0040}$	$0.0099^{+0.0051}_{-0.0037}$
$\chi_{min}^2$	424.141	388.239

### III. RESULTS

We perform an MCMC likelihood analysis [72] to obtain  $\mathcal{O}(10^6)$  samples for each set of results presented in this paper. We assume flat priors for all the parameters, and allow ranges of the parameters wide enough such that further increasing the allowed ranges has no impact on the results. The chains typically have worst e-values (the variance(mean)/mean(variance) of 1/2 chains) much smaller than 0.01, indicating convergence.

In the following, we will discuss the effects of varying  $\beta$  and different light-curve fitters on the SNLS3 constraints on the HDE model, respectively.

#### A. The effects of varying $\beta$

In this subsection, we discuss the effects of varying  $\beta$ . As mentioned above, to explore the evolution of  $\beta$ , we study the case of constant  $\alpha$  and linear  $\beta(z) = \beta_0 + \beta_1 z$ ; for comparison, the case of constant  $\alpha$  and constant  $\beta$  is also taken into account. For simplicity, here we only use the SN data from the ‘‘Combined’’ set. In Table I, we make a comparison for the fitting results of constant  $\beta$  and linear  $\beta(z)$  cases, where the SN(Combined)+CMB+GC data are used. From this table, we can see that varying  $\beta$  can significantly improve the fitting results: adding a parameter of  $\beta$  can reduce the values of  $\chi_{min}^2$  by  $\sim 35$ . This result is consistent with the conclusion of [52], where the  $\Lambda$ CDM, the  $w$ CDM, and the CPL models are considered in that paper. Therefore, the evolution of  $\beta$  is independent of the cosmological models in the background. This shows that the importance of considering  $\beta$ 's evolution in the cosmology-fits.

Let us discuss the effects of varying  $\beta$  with more details. In Fig. 1, using SN(Combined)+CMB+GC data, we plot the joint 68% and 95% confidence contours for  $\{\beta_0, \beta_1\}$  (top panel), and the 68%, 95%, and 97% confidence constraints for the reconstructed evolution of  $\beta(z)$  (bottom panel), for the linear  $\beta(z)$  case. For comparison, we also show the best-fit result of constant  $\beta$  case in the

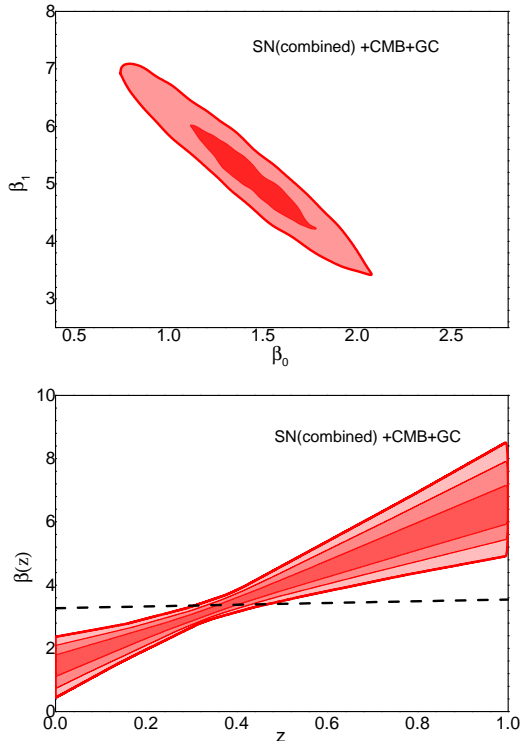


FIG. 1: The joint 68% and 95% confidence contours for  $\{\beta_0, \beta_1\}$  (top panel) and the 68%, 95%, and 97% confidence constraints for  $\beta(z)$  (bottom panel), given by the SN(Combined)+CMB+GC data. For comparison, the best-fit result of constant  $\beta$  case is also shown in the bottom panel.

bottom panel. The top panel shows that  $\beta_1 > 0$  at a high confidence level (CL), while the bottom panel shows that  $\beta(z)$  rapidly increases with  $z$ . In other words, according to this figure, we find the deviation of  $\beta$  from a constant at  $5\sigma$  CL. This result is consistent with that of Refs. [51] and [52], and further confirms that the evolution of  $\beta$  is insensitive to the DE models considered and should be taken into account seriously in the cosmology-fits.

In Fig. 2, using the same data, we plot the 1D marginalized probability distributions of  $\Omega_{m0}$ ,  $c$ , and  $h$ , for both the constant  $\beta$  and linear  $\beta(z)$  cases. We find that varying  $\beta$  yields a larger  $\Omega_{m0}$ , a larger  $c$  and a smaller  $h$ .

In Fig. 3, we plot the joint 68% and 95% confidence contours for  $\{\Omega_{m0}, c\}$ ,  $\{\Omega_{m0}, h\}$ , and  $\{c, h\}$ . Again, we see that varying  $\beta$  yields a larger  $\Omega_{m0}$ , a larger  $c$ , and a smaller  $h$ , compared to the case of assuming a constant  $\beta$ . Moreover, we also find that, for these two cases, the  $2\sigma$  CL ranges of parameter space are quite different. This means that ignoring the evolution of  $\beta$  may cause systematic bias. In addition, it is clear that  $\Omega_{m0}$  and  $h$  are strongly anti-correlated; this is also consistent with the cases of the  $\Lambda$ CDM,  $w$ CDM, and CPL models [52].

In Fig. 4, we plot the 68% confidence constraints for the reconstructed EOS  $w(z)$  of HDE. From this figure, we see that varying  $\beta$  yields a larger  $w(z)$ : for the constant

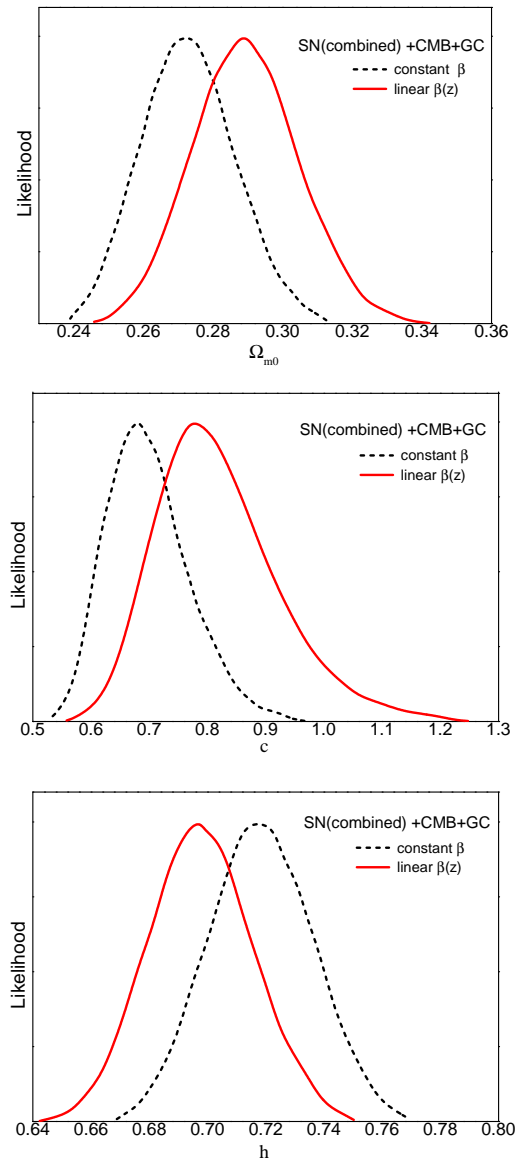


FIG. 2: The 1D marginalized probability distributions of  $\Omega_{m0}$  (top panel),  $c$  (central panel), and  $h$  (bottom panel), given by the SN(Combined)+CMB+GC data. Both the results of constant  $\beta$  and linear  $\beta(z)$  cases are presented.

$\beta$  case,  $w(z=0) < -1$  at  $1\sigma$  CL; while for the linear  $\beta(z)$  case,  $w(z=0)$  is still consistent with  $-1$  at  $1\sigma$  CL. Therefore, the results from varying  $\beta$  case are in better agreement with a cosmological constant than those from the constant  $\beta$  case.

## B. The effects of different light-curve fitters

In this subsection, we discuss the effects of different light-curve fitters (including “Combined”, “SALT2”, and “SiFTO”). Notice that we also include the CMB and the GC data. For simplicity, here we only consider the case

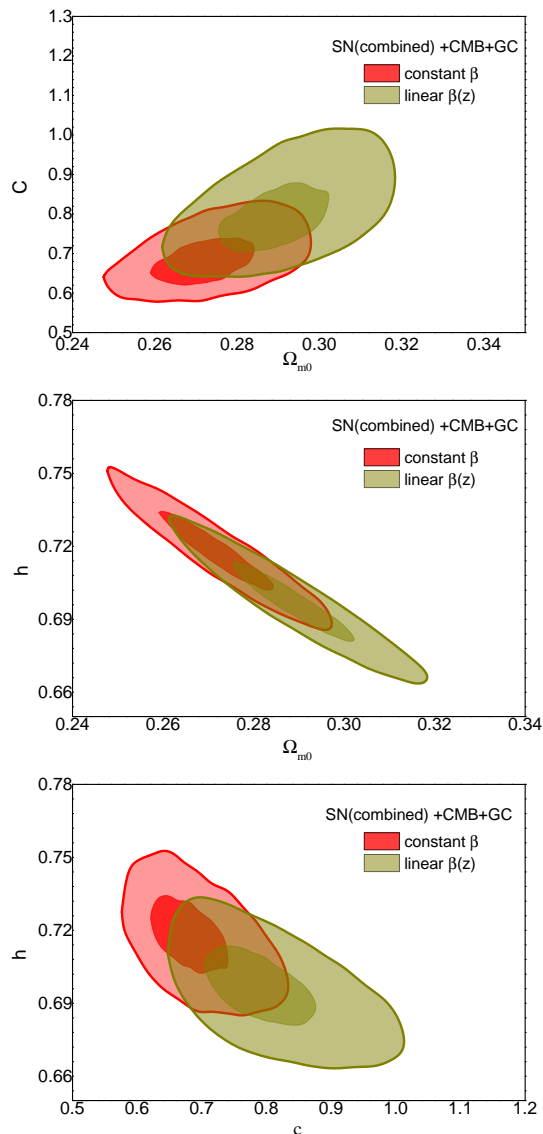


FIG. 3: The joint 68% and 95% confidence contours for  $\{\Omega_{m0}, c\}$  (top panel),  $\{\Omega_{m0}, h\}$  (central panel), and  $\{c, h\}$  (bottom panel), given by the SN(Combined)+CMB+GC data. Both the results of constant  $\beta$  and linear  $\beta(z)$  cases are presented.

of linear  $\beta(z)$ . In Table II, we make a comparison for the fitting results given by the “Combined”, the “SALT2”, and the “SiFTO” SN sets. An obvious feature of this table is that the differences of various cosmological parameters are very small, while the differences of SN parameters (including  $\alpha$ ,  $\beta_0$  and  $\beta_1$ ) are a little larger. In the following, we will discuss this issue with more details.

Firstly, let us focus on the evolution of  $\beta$ . In Fig. 5, we plot the 68% confidence constraints for the reconstructed evolution of  $\beta(z)$  in the HDE model, given by the “Combined”, the “SALT2”, and the “SiFTO” SN sets. It can be seen that the evolution of  $\beta$  given by the “Combined” set is very close to that given by the “SiFTO” SN set; in contrast, the “SALT2” set give a different  $\beta$ ’s evolution,

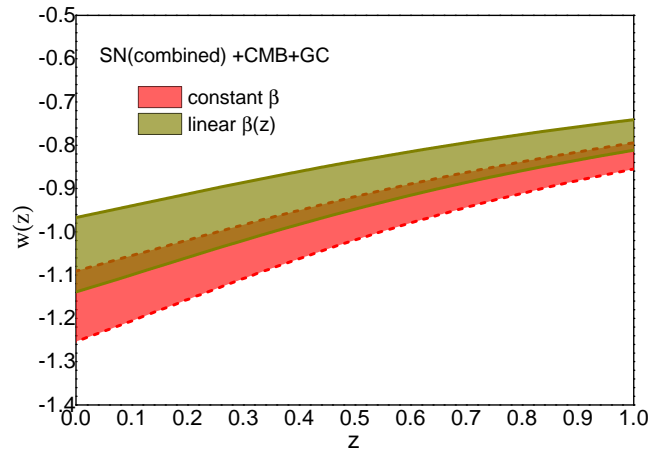


FIG. 4: The 68% confidence constraints for the EOS  $w(z)$  of HDE, given by the SN(Combined)+CMB+GC data. Both the results of constant  $\beta$  and linear  $\beta(z)$  cases are presented.

TABLE II: A comparison for the fitting results given by the “Combined”, the “SALT2”, and the “SiFTO” SN sets. The linear  $\beta(z)$  is adopted in the analysis.

Parameter	Combined	SALT2	SiFTO
$\alpha$	$1.416^{+0.097}_{-0.095}$	$1.572^{+0.194}_{-0.151}$	$1.370^{+0.058}_{-0.081}$
$\beta_0$	$1.403^{+0.359}_{-0.312}$	$1.996^{+0.285}_{-0.249}$	$1.438^{+0.343}_{-0.359}$
$\beta_1$	$5.167^{+0.971}_{-0.967}$	$3.878^{+0.774}_{-0.835}$	$5.275^{+0.947}_{-0.894}$
$\Omega_{m0}$	$0.288^{+0.015}_{-0.013}$	$0.285^{+0.017}_{-0.012}$	$0.284^{+0.018}_{-0.013}$
$c$	$0.768^{+0.112}_{-0.068}$	$0.751^{+0.081}_{-0.091}$	$0.745^{+0.105}_{-0.068}$
$h$	$0.698^{+0.017}_{-0.017}$	$0.701^{+0.017}_{-0.018}$	$0.702^{+0.017}_{-0.019}$
$\omega_b$	$0.02230^{+0.00027}_{-0.00029}$	$0.02235^{+0.00023}_{-0.00033}$	$0.02233^{+0.00024}_{-0.00032}$
$\Omega_{k0}$	$0.0099^{+0.0051}_{-0.0037}$	$0.0101^{+0.0040}_{-0.0043}$	$0.0091^{+0.0052}_{-0.0037}$

whose increasing rate is a little smaller. But for all these three cases, the trends of  $\beta(z)$  are still the same, and all of them deviate from a constant at a high CL. This result is consistent with the fixed cosmology background case (see Figure 5 of [51]). Thus, it further confirms that the evolution of  $\beta$  is insensitive to the light-curve fitters used to derive the SNLS3 sample, or the cosmological model used in the background.

Then, let us discuss the effects of different SNLS3 samples on parameter estimation. In Fig. 6, we plot the 1D marginalized probability distributions of  $\Omega_{m0}$ ,  $c$ , and  $h$ , given by the “Combined”, the “SALT2”, and the “SiFTO” SN sets. It can be seen that the results given by the “SALT2” and the “SiFTO” SN sets are very close, while the “Combined” set yields a larger  $\Omega_{m0}$ , a larger  $c$ , and a smaller  $h$ . However, compared to the effects of varying  $\beta$  (see Fig. 2), the effects of different light-curve fitters are much smaller.

In Fig. 7, we plot the joint 68% and 95% confidence contours for  $\{\Omega_{m0}, c\}$ , given by the three SNLS3 samples. It is found that the results given by the “SALT2” and the “SiFTO” SN sets are very close, while the results given

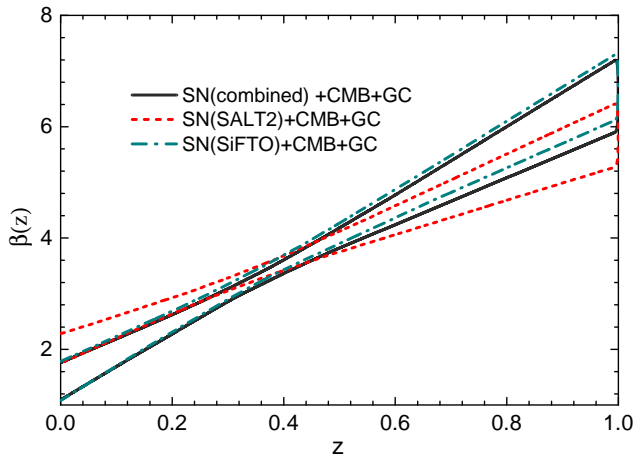


FIG. 5: The 68% confidence constraints for the evolution of  $\beta(z)$  in the HDE model, given by the “Combined”, the “SALT2”, and the “SiFTO” SN sets.

by the “Combined” set are a little different. Moreover, compared to Fig. 3, it can be seen that the effects of different light-curve fitters are much smaller than those of varying  $\beta$ .

At last, let us discuss the effects of different light-curve fitters on the EOS  $w(z)$ . In Fig. 8, we make a comparison for the 68% confidence constraints for the EOS  $w(z)$  of HDE, given by the “Combined”, the “SALT2”, and the “SiFTO” SN sets. Again, we find that the results given by the “SALT2” and the “SiFTO” SN sets are very close; beside, the “Combined” set gives a larger  $w(z)$ . All these three SN sets yield a  $w(z=0)$  that is consistent with  $-1$  at  $1\sigma$  CL. So compared to the differences between constant  $\beta$  and time-varying  $\beta(z)$  cases (see Fig. 4), the effects of different light-curve fitters are very small.

#### IV. DISCUSSION AND SUMMARY

As is well known, at current stage, systematic uncertainties of SNe Ia have become the key issue of SN cosmology. One of the most important systematic uncertainties for SNe Ia is the potential SN evolution, i.e., the possibility of the evolution of  $\alpha$  and  $\beta$  with redshift  $z$  [47–50]. In [51], using the SNLS3 data and MCMC technique, Wang & Wang found that  $\alpha$  is still consistent with a constant, but there is a strong evidence for the evolution of  $\beta$ . In [52], considering the cosmological constant, the constant  $w$ , and the non-constant  $w$  models, Wang, Li & Zhang showed that a time-varying  $\beta$  has significant impact on parameter estimation; in addition, it was found that considering the evolution of  $\beta$  is helpful to reduce the tension between SN and other cosmological observations.

In this paper, we have explored the evolution of  $\beta$  and its effects on parameter estimation in the HDE model. To break the degeneracy between various model parameters,

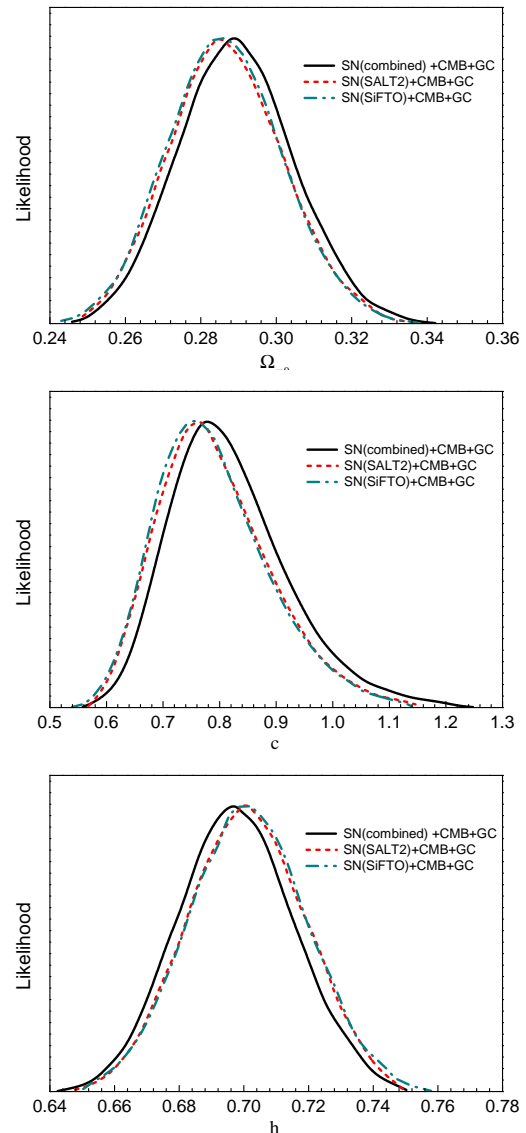


FIG. 6: The 1D marginalized probability distributions of  $\Omega_{m0}$  (top panel),  $c$  (central panel), and  $h$  (bottom panel), given by the “Combined”, the “SALT2”, and the “SiFTO” SN sets.

we have taken into account the latest Planck distance priors data [60], as well as the latest GC data extracted from SDSS DR7 [61] and BOSS [62]. In addition, we have also studied the effects of different light-curve fitters on parameter estimation.

We find that, for the HDE model,  $\beta$  deviates from a constant at the  $5\sigma$  CL (see Fig. 1). Moreover, we find that adding a parameter of  $\beta$  can reduce the values of  $\chi^2$  by  $\sim 35$  (see Table I). These results are consistent with those of the  $\Lambda$ CDM, the  $w$ CDM, and the CPL models. This implies that the evolution of  $\beta$  is insensitive to the DE models in the background and should be taken into account seriously in the cosmology-fits.

Compared to the constant  $\beta$  case, varying  $\beta$  yields a larger  $\Omega_{m0}$ , a larger  $c$  and a smaller  $h$  (see Figs. 2 and

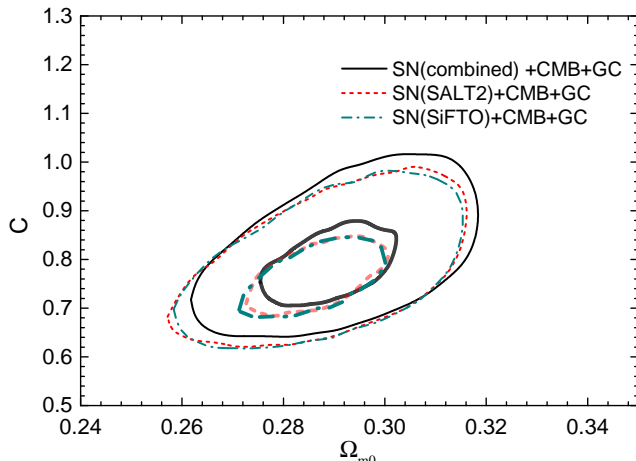


FIG. 7: The joint 68% and 95% confidence contours for  $\{\Omega_{m0}, c\}$ , given by the “Combined”, the “SALT2”, and the “SiFTO” SN sets.

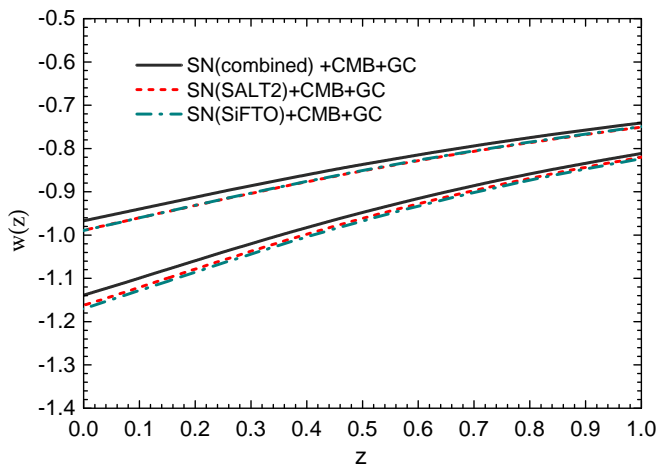


FIG. 8: The 68% confidence constraints for the EOS  $w(z)$  of HDE, given by the “Combined”, the “SALT2”, and the “SiFTO” SN sets.

3). For these two cases, the  $2\sigma$  CL ranges of parameter space are quite different. This indicates that ignoring the evolution of  $\beta$  may cause systematic bias.

Varying  $\beta$  also yields a larger  $w(z)$ : for the constant  $\beta$  case,  $w(z=0) < -1$  at  $1\sigma$  CL; while for the linear  $\beta(z)$  case,  $w(z=0)$  is consistent with  $-1$  at  $1\sigma$  CL (see Fig. 4). So, the results from the varying  $\beta$  SN data are in better agreement with a cosmological constant than those from the constant  $\beta$  SN data.

We find that the evolution of  $\beta$  given by the “Combined” and the “SiFTO” SN sets are very close; while the “SALT2” set will give a different  $\beta$ ’s evolution, whose increasing rate is a little smaller (see Fig. 5). We also find that the cosmology-fits results given by the “SALT2” and the “SiFTO” SN sets are very close, while the “Combined” set yields a larger  $\Omega_{m0}$ , a larger  $c$ , a smaller  $h$ , and a larger  $w(z)$  (see Figs. 6, 7 and 8). However, compared to the differences between constant  $\beta$  and time-varying  $\beta(z)$  cases, the effects of different light-curve fitters are very small.

In this paper, only the potential SN evolution is taken into account. Some other factors, such as the evolution of  $\sigma_{int}$  [63], may also cause the systematic uncertainties for SNe Ia. This issue deserves further study in future.

### Acknowledgments

We thank Yun-He Li for helpful discussions. We are also grateful to Alex Conley for providing us with the SNLS3 covariance matrices that allow redshift-dependent  $\alpha$  and  $\beta$ . We acknowledge the use of CosmoMC. This work is supported by the National Natural Science Foundation of China (Grants No. 10975032 and No. 11175042) and by the National Ministry of Education of China (Grants No. NCET-09-0276 and No. N120505003).

- 
- [1] A. G. Riess *et al.*, *AJ*. **116**, 1009 (1998); S. Perlmutter *et al.*, *ApJ*. **517**, 565 (1999).
- [2] D. N. Spergel *et al.*, *ApJS* **148**, 175 (2003); C. L. Bennet *et al.*, *ApJS*. **148**, 1 (2003); D. N. Spergel *et al.*, *ApJS* **170**, 377 (2007); L. Page *et al.*, *ApJS* **170**, 335 (2007); G. Hinshaw *et al.*, *ApJS* **170**, 263 (2007).
- [3] M. Tegmark *et al.*, *Phys. Rev. D* **69**, 103501 (2004); *ApJ* **606**, 702 (2004); *Phys. Rev. D* **74**, 123507 (2006).
- [4] E. Komatsu *et al.*, *ApJS*. **180**, 330 (2009); E. Komatsu *et al.*, *ApJS*. **192**, 18 (2011).
- [5] W. J. Percival *et al.*, *MNRAS* **401**, 2148 (2010); A. G. Sanchez, *et al.*, arXiv:1203.6616, *MNRAS* accepted.
- [6] M. Drinkwater *et al.*, *MNRAS* **401**, 1429 (2010); C. Blake *et al.*, arXiv:1108.2635, *MNRAS* accepted.
- [7] A. G. Riess *et al.*, *ApJ*. **730**, 119 (2011).
- [8] P. J. E. Peebles and B. Ratra, *ApJ* **325**, L17 (1988); C. Wetterich, *Nucl. Phys. B* **302**, 668 (1988); R. R. Caldwell, R. Dave and P. J. Steinhardt, *Phys. Rev. Lett.* **80**, 1582 (1998); I. Zlatev, L. Wang and P. J. Steinhardt, *Phys. Rev. Lett.* **82**, 896 (1999).
- [9] R. R. Caldwell, *Phys. Lett. B* **545**, 23 (2002); S. M. Carroll, M. Hoffman and M. Trodden, *Phys. Rev. D* **68**, 023509 (2003); R. R. Caldwell, M. Kamionkowski and N. N. Weinberg, *Phys. Rev. Lett.* **91**, 071301 (2003).
- [10] C. Armendariz-Picon, T. Damour and V. Mukhanov, *Phys. Lett. B* **458**, 209 (1999); C. Armendariz-Picon, V. Mukhanov and P. J. Steinhardt, *Phys. Rev. D* **63**, 103510 (2001); T. Chiba, T. Okabe and M. Yamaguchi, *Phys. Rev. D* **62**, 023511 (2000).
- [11] A. Y. Kamenshchik, U. Moschella and V. Pasquier, *Phys. Lett. B* **511**, 265 (2001); M. C. Bento, O. Bertolami and A. A. Sen, *Phys. Rev. D* **66**, 043507 (2002).
- [12] X. Zhang, F. Q. Wu and J. Zhang, *JCAP* **01**, 003 (2006); K. Liao, Y. Pan and Z. H. Zhu, *Res. Astron. Astrophys.* **13**, 159 (2013).
- [13] T. Padmanabhan, *Phys. Rev. D* **66**, 021301 (2002); J. S.

- Bagla, H. K. Jassal, and T. Padmanabhan, *Phys. Rev. D* **67**, 063504 (2003).
- [14] H. Wei, R. G. Cai, and D. F. Zeng, *Class. Quant. Grav.* **22**, 3189 (2005); H. Wei, and R. G. Cai, *Phys. Rev. D* **72**, 123507 (2005); H. Wei, N. Tang, and S. N. Zhang, *Phys. Rev. D* **75**, 043009 (2007).
- [15] W. Zhao and Y. Zhang, *Class. Quant. Grav.* **23**, 3405 (2006); T. Y. Xia and Y. Zhang, *Phys. Lett. B* **656**, 19 (2007); S. Wang, Y. Zhang and T. Y. Xia, *JCAP* **10**, 037 (2008); S. Wang and Y. Zhang, *Phys. Lett. B* **669**, 201 (2008).
- [16] X. Zhang, *Phys. Lett. B* **648**, 1 (2007); *Phys. Rev. D* **74**, 103505 (2006); J. Zhang, X. Zhang and H. Liu, *Phys. Lett. B* **651**, 84 (2007); *Eur. Phys. J. C* **54**, 303 (2008); X. Zhang, *Phys. Rev. D* **79**, 103509 (2009).
- [17] D. Comelli, M. Pietroni and A. Riotto, *Phys. Lett. B* **571**, 115 (2003); X. Zhang, *Mod. Phys. Lett. A* **20**, 2575 (2005); *Phys. Lett. B* **611**, 1 (2005).
- [18] K. Freese et al., *Nucl. Phys. B* **287**, 797 (1987); A. Linde, in *Three hundred years of gravitation*, (Eds.: Hawking, S.W. and Israel, W., Cambridge Univ. Press, 1987), 604; J. A. Frieman, C. T. Hill, A. Stebbins, and I. Waga, *Phys. Rev. Lett.* **75**, 2077 (1995); M. Chevallier and D. Polarski, *Int. J. Mod. Phys. D* **10**, 213 (2001); E. V. Linder, *Phys. Rev. Lett.* **90** 091301 (2003); D. Huterer and G. Starkman, *Phys. Rev. Lett.* **90**, 031301 (2003); D. Huterer and A. Cooray, *Phys. Rev. D* **71**, 023506 (2005); A. Shafieloo, V. Sahni and A. A. Starobinsky, *Phys. Rev. D* **80**, 101301(R) (2009).
- [19] Y. Wang and M. Tegmark, *Phys. Rev. Lett.* **92**, 241302 (2004); Y. Wang, and K. Freese, *Phys. Lett. B* **632**, 449 (2006); Y. Wang and P. Mukherjee, *ApJ*. **650**, 1 (2006); Y. Wang and P. Mukherjee, *Phys. Rev. D* **76**, 103533 (2007); Y. Wang, *Phys. Rev. D* **78**, 123532 (2008).
- [20] Y. Wang and M. Tegmark, *Phys. Rev. D* **71**, 103513 (2005);
- [21] Q. G. Huang, M. Li, X. D. Li and S. Wang, *Phys. Rev. D* **80**, 083515 (2009); S. Wang, X. D. Li and M. Li, *Phys. Rev. D* **82**, 103006 (2010); M. Li, X. D. Li and X. Zhang, *Sci. China Phys. Mech. Astron.* **53**, 1631 (2010); S. Wang, X. D. Li and M. Li, *Phys. Rev. D* **83**, 023010 (2011); X. D. Li et al., *JCAP* **07**, (2011) 011; J. Z. Ma and X. Zhang, *Phys. Lett. B* **699**, 233 (2011); H. Li and X. Zhang, *Phys. Lett. B* **713**, 160 (2012); X. D. Li et al., *Sci. China Phys. Mech. Astron.* **55**, 1330 (2012).
- [22] V. Sahni and S. Habib, *Phys. Rev. Lett.* **81**, 1766 (1998).
- [23] L. Parker and A. Raval, *Phys. Rev. D* **60**, 063512 (1999).
- [24] G. Dvali, G. Gabadadze and M. Porrati, *Phys. Lett. B* **485**, 208 (2000).
- [25] S. Nojiri, S. D. Odintsov, and M. Sasaki, *Phys. Rev. D* **71**, 123509 (2005).
- [26] A. Nicolis, R. Rattazzi, and E. Trincherini, *Phys. Rev. D* **79**, 064036 (2009).
- [27] W. Hu and I. Sawicki, *Phys. Rev. D* **76**, 064004 (2007); A. A. Starobinsky, *J. Exp. Theor. Phys. Lett.* **86**, (2007) 157.
- [28] G. R. Bengochea and R. Ferraro, *Phys. Rev. D* **79**, 124019 (2009); E. V. Linder, *Phys. Rev. D* **81**, (2010) 127301.
- [29] T. Harko, F. S. N. Lobo, S. Nojiri and S. D. Odintsov, *Phys. Rev. D* **84**, 024020 (2011).
- [30] E. J. Copeland, M. Sami and S. Tsujikawa, *Int. J. Mod. Phys. D* **15**, 1753 (2006).
- [31] J. Frieman, M. Turner and D. Huterer, *Ann. Rev. Astron. Astrophys* **46**, 385 (2008).
- [32] E. V. Linder, *Rept. Prog. Phys.* **71**, 056901 (2008).
- [33] R. R. Caldwell and M. Kamionkowski, *Ann. Rev. Nucl. Part. Sci.* **59**, 397 (2009).
- [34] J.-P. Uzan, arXiv:0908.2243.
- [35] S. Tsujikawa, arXiv:1004.1493.
- [36] S. Nojiri and S. D. Odintsov, *Phys. Rept.* **505**, 59 (2011).
- [37] M. Li, X. D. Li, S. Wang and Y. Wang, *Commun. Theor. Phys.* **56**, 525 (2011).
- [38] T. Clifton, P. G. Ferreira, A. Padilla and C. Skordis, *Phys. Rept.* **513**, 1 (2012).
- [39] Y. Wang, *Dark Energy*, Wiley-VCH (2010).
- [40] M. Kowalski, et al., *ApJ*. **686**, 749 (2008).
- [41] M. Hicken, et al., *ApJ*. **700**, 1097 (2009); M. Hicken, et al., *ApJ*. **700**, 331 (2009).
- [42] R. Amanullah, et al., *ApJ*. **716**, 712 (2010).
- [43] N. Suzuki, et al., *ApJ* **746**, 85 (2012).
- [44] J. Guy, et al., *A&A*, **523**, 7 (2010).
- [45] A. Conley, et al., *ApJS*. 192 1 (2011) – **C11**
- [46] M. Sullivan, et al., arXiv:1104.1444.
- [47] R. Kessler, et al., *ApJS*. **185**, 32 (2009).
- [48] G. Mohlabeng and J. Ralston, arXiv:1303.0580.
- [49] D. Scolnic, et al., arXiv:1306.4050, *ApJ* in press.
- [50] D. Scolnic, et al., arXiv:1310.3824.
- [51] S. Wang and Y. Wang, *Phys. Rev. D* **88**, 043511 (2013).
- [52] S. Wang, Y. H. Li and X. Zhang, arXiv:1310.6109.
- [53] E. Witten, arXiv:hep-ph/0002297.
- [54] G. 't Hooft, gr-qc/9310026; L. Susskind, *J. Math. Phys.* **36**, 6377 (1995).
- [55] A. Cohen, D. Kaplan, A. Nelson, *Phys. Rev. Lett.* **82**, 4971 (1999).
- [56] M. Li, *Phys. Lett. B* **603**, 1 (2004).
- [57] Y. H. Li, S. Wang, X. D. Li and X. Zhang, *JCAP* **02**, 033 (2013).
- [58] Q. G. Huang and M. Li, *JCAP* **03**, 001 (2005); X. Zhang, *Int. J. Mod. Phys. D* **14**, 1597 (2005); B. Chen, M. Li and Y. Wang, *Nucl. Phys. B* **774**, 256 (2007); J. F. Zhang, X. Zhang and H. Y. Liu, *Phys. Lett. B* **659**, 26 (2008); *Eur. Phys. J. C* **52**, 693 (2007); M. Li, C. S. Lin and Y. Wang, *JCAP* **05**, 023 (2008); Y. Z. Ma and X. Zhang, *Phys. Lett. B* **661**, 239 (2008); M. Li et al., *Commun. Theor. Phys.* **51**, 181 (2009); M. Li, R. X. Miao and Y. Pang, *Phys. Lett. B* **689**, 55 (2010); M. Li and Y. Wang, *Phys. Lett. B* **687**, 243 (2010); Y. G. Gong and T. J. Li, *Phys. Lett. B* **683**, 241 (2010); X. Zhang, *Phys. Lett. B* **683**, 81 (2010).
- [59] Q. G. Huang and Y. G. Gong, *JCAP* **08**, 006 (2004); X. Zhang and F. Q. Wu, *Phys. Rev. D* **72**, 043524 (2005); *Phys. Rev. D* **76**, 023502 (2007); Z. Chang, F. Q. Wu and X. Zhang, *Phys. Lett. B* **633**, 14 (2006); Y. Z. Ma, Y. Gong and X. L. Chen, *Eur. Phys. J. C* **60**, 303 (2009); M. Li et al., *JCAP* **06**, 036 (2009); M. Li et al., *JCAP* **12**, 014 (2009); Z. H. Zhang et al., *JCAP* **06**, 009 (2012); M. Li et al., *JCAP* **09**, 021 (2013).
- [60] Y. Wang and S. Wang, *Phys. Rev. D* **88**, 043522 (2013).
- [61] C. H. Chuang and Y. Wang, *MNRAS*, **426**, 226 (2012).
- [62] C. H. Chuang, et al., arXiv:1303.4486.
- [63] A. Kim, arXiv:1101.3513; J. Marriner, et al., arXiv:1107.4631.
- [64] Y. Wang, *ApJ* **536**, 531 (2000).
- [65] Y. Wang and P. Mukherjee, *ApJ*. **606**, 654 (2004).
- [66] Y. Wang, *JCAP*, **03**, 005 (2005).
- [67] Y. Wang, C. H. Chuang and P. Mukherjee, *Phys. Rev. D* **85**, 023517 (2012).

- [68] Y. Wang and P. Mukherjee, Phys. Rev. D, **76**, 103533 (2007).
- [69] Y. Wang, Phys. Rev. D **77**, 123525 (2008).
- [70] W. Hu and N. Sugiyama, ApJ, **471**, 542 (1996).
- [71] D. Eisenstein and W. Hu, ApJ, **496**, 605 (1998).
- [72] A. Lewis and S. Bridle, Phys. Rev. D **66**, 103511 (2002).